Biologia (2018) 73:773–786
https://doi.org/10.2478/s11756-018-0088-4

ORIGINAL ARTICLE

Cephalic specializations in relation to a second set of jaws in muraenids

Soheil Eagderi[1] · Dominique Adiaens[2]

Received: 23 February 2018 / Accepted: 27 June 2018 / Published online: 16 July 2018

Abstract

The Muraenidae, one of the largest clades within the anguilliform fishes, exhibit an innovative feeding mechanism that allows them to transport large prey items from the oral jaw all the way back towards the esophagus, using highly specialised pharyngeal jaws. This study was conducted to show the degree to what trade-offs in muraenids may have arisen in the oral feeding apparatus, in relation to this pharyngeal transport system. Hence, the head musculoskeletal features of *Anarchias allardicei* (Uropterygiinae: Muraenidae) and *Gymnothorax prasinus* (Muraeninae: Muraenidae) were compared with that of a closely-related out-group with a hydraulic based prey transport, *Ariosoma gilberti* (Bathymyrinae: Congridae) by providing a detailed description of the cranial osteology and myology of *A. allardicei* and *G. prasinus*. The result showed that this innovative feeding mechanism may be linked to many cephalic modifications such as, stout and robust neurocranial elements, elongated lower jaw as result of the posterior position of the quadrato-mandibular articulation, enlarged teeth of oral jaws and premaxillo-ethmovomeral complex, reduction in the moveable cranial bones and their muscular connections, hypertrophied adductor mandibulae muscle complex, presence of the quadrato-maxillary and preoperculo-angular ligaments, connection of the quadrate to the A2 tendon of the adductor mandibulae complex and caudoventral orientation of the fibers of the large A3 section of the adductor mandibulae complex.

Keywords Cranial · Osteology · Myology · *Anarchias allardicei* · *Gymnothorax prasinus* · *Ariosoma gilberti*

Introduction

The eels of the Anguilliformes are an order comprising 9 families, 159 genera, and about 938 species, thereby forming the most diverse order within the Elopomorpha (Nelson et al. 2016). The Muraenidae, one of the largest clades within the anguilliforms and known as morays, include about 200 species within more than 16 genera (Böhlke et al. 1989; Nelson et al. 2016). Two monophyletic subfamilies are recognized, i.e. Uropterygiinae and Muraeninae (Obermiller and Pfeiler 2003; Wang et al. 2003; Lopez et al. 2007; Nelson et al. 2016). Typically morays are shallow-water reef and crevice-dwelling eels. They are carnivores and their abundance and biomass within shallow water reef in general is much greater than casually perceived (Böhlke et al. 1989; Santos and Castro 2003). The muraenids bear an evolutionary novel feeding mechanism, which may explain their evolutionary success (Mehta and Wainwright 2007a). Using their pharyngeal jaws, morays are capable to transport captured large prey from the oral jaws all the way back towards the esophagus (Mehta and Wainwright 2007a).

In contrast to the morays, most ray-finned fishes use a suction-induced flow of water to move prey from the oral jaws to the pharyngeal jaws (Gillis and Lauder 1995; Mehta and Wainwright 2007a, 2008). Therefore, presence of the specialized mechanical transport system in morays provides an opportunity to better understand morphological changes on their head musculoskeletal system in relation to a novel feeding behavior and this within a proper phylogenetic framework. Hence, by comparing the cephalic morphology of representatives of lineage both within morays, such as uropterygiines and muraenines, as well as representative of a closely-related anguilliform family that still possess the plesiomorphic hydraulic based prey transport, the morphological changes in relation to this specialization may better understood within a functional context.

✉ Soheil Eagderi
soheil.eagderi@ut.ac.ir

[1] Department of Fisheries, Faculty of Natural Resources, University of Tehran, Karaj, Iran

[2] Ghent University, Evolutionary Morphology of Vertebrates, K.L. Ledeganckstraat 35, 9000 Ghent, Belgium

This study aimed to better understand the evolutionary changes in head morphology that are associated with the novel mechanical transport system in moray eels. Hence, we provide a detailed description of the cranial myology and osteology of representatives of the two muraenid subfamilies, i.e. *Anarchias allardicei* (Jordan and Starks, 1906) (Uropterygiinae: Muraenidae) and *Gymnothorax prasinus* (Richardson, 1848) (Muraeninae: Muraenidae), and compare their head musculoskeletal features with that of a closely-related anguilliform family that is characterised by using a hydraulic based prey transport system: *Ariosoma gilberti* (Ogilby, 1898) (Bathymyrinae: Congridae). This comparison was done to reveal to what degree tradeoffs may have arisen on the overall head morphology of morays, especially focusing on the oral jaws, in relation to this pharyngeal transport system i.e. how may a highly specialized pharyngeal mechanical transport system in morays have affected the evolutionary changes in the head musculoskeletal system? The choice for *A. gilberti* as an outgroup is based on a single most parsimonious tree of elopomorph fishes, using the combined data of mitochondrial 12S ribosomal RNA sequences, which supports the monophyly of the clade comprising Muraenidae and Bathymyrinae (Congridae) (Obermiller and Pfeiler 2003).

Material and methods

For the anatomical description, four alcohol-preserved specimens of *G. prasinus* (I.28736–024 and I.20095–031) and eight specimens of *A. allardicei* (I.17102–063 and UF 318044) obtained from the Australian Museum were examined. The specimens had the following size: *G. prasinus* (GP)1: 437 mm TL (Total Length); GP2: 385.5 mm TL; GP3: 497 mm TL; GP4: 447.2 TL; *A. allardicei* (AA)1: 99 mm TL; AA2: 101 mm TL; AA3: 108 mm TL; AA4: 107 mm TL; AA5: 110 mm TL; AA6: 146 mm TL; AA7: 129 mm TL; AA8: 136 mm TL. One specimens of each species (GP2 and AA1) were cleared and stained with Alizarin red S and Alcian blue according to the protocol of Hanken and Wassersug (1981) for osteological examinations. Dissections with muscle fiber staining according to Bock and Shear (1972) were performed. Specimens were studied using a stereoscopic microscope (Olympus SZX-7) equipped with a camera lucida.

The musculature terminology follows Winterbottom (1974), De Schepper et al. (2005) and Mehta and Wainwright (2007a). The circumorbital bones of the cephalic lateral line system follow Adriaens et al. (1997). Terminology of cranial skeletal elements follows Nelson (1966), Böhlke (1989) and Rojo (1991). The epiotic of teleosts is termed "epioccipital", thereby following Patterson (1975). The terminology of scarf joint follows Hildebrand (1995). The cranial osteology and myology of *A. gilberti* (Bathymyrinae: Congridae) has been described in detail by Eagderi and Adriaens (2014).

Results

Cranial osteology

Neurocranium The general morphology of the skull of *G. prasinus* and *A. allardicei* is very similar. Their neurocranium are stout and taper from the otic region towards the posterior part of the premaxillo-ethmovomeral complex. Their ethmoid region comprises the premaxillo-ethmovomeral complex and nasals (Figs. 1a and 2a). In both species, the olfactory rosette is located dorsal to the rostrum, with a vertical wall of the premaxillo-ethmovomeral complex separating left from right nasal cavities (Figs. 1a and 2a). The premaxillo-ethmovomeral complex of *G. prasinus* and *A. allardicei* is relatively short and shovel-like in a ventral view (Figs. 3 and 4b). In *G. prasinus*, it bilaterally bears caudally directed struts (Fig. 3), whereas those of *A. allardicei* are the small maxillary articular facets (Fig. 4). Both species bear some teeth on the posterior process of the premaxillo-ethmovomeral complex, separated from the anterior teeth by an edentulous zone (Figs. 3b and 4b). This anterior dentition in *G. prasinus* comprises three rows of large, curved teeth with small teeth between the teeth of the two lateral rows (Fig. 3b). Its posterior teeth are shorter and arranged in a single row. In *A. allardicei*, the anterior part of the premaxillo-ethmovomeral complex contains of few pointed teeth with a row of smaller teeth bordering the bone complex (Fig. 4b). Also, some small teeth are scattered among its large teeth (Fig. 4b). Teeth on the posterior part are arranged in a single row as in *G. prasinus* but only with three pointed teeth (Fig. 4b).

The orbital region of *G. prasinus* consists of the adnasal, lacrimal, infraorbitals, supraorbitals, frontal, basisphenoid, parasphenoid and pterosphenoid bones, whereas that of *A. allardicei* lacks the supraorbital and adnasal bones. In *G. prasinus*, the frontal bears an anterodorsal tube-like process with dorsal and lateral openings connected to the temporal canal (Fig. 1a). Also, a small fontanel is present between two frontals (Fig. 3a). In *A. allardicei*, the frontal anteriorly bears a groove, anterior to entrance of the temporal canal (Figs. 2a and 4a). A small canal ventral to this frontal groove posteriorly connects to the temporal canal (Fig. 2a). The frontals of *A. allardicei* overlap with the anterior half of the parietals (Fig. 4a), whereas those of *G. prasinus* form an interdigitating suture. The basisphenoid forms the posterior wall of a small orbit in *G. prasinus* and *A. allardicei* (Figs. 1a and 2a). In both muraenids, the basisphenoid bears the optic foramen on its lateral face (Figs. 1a and 2a). The olfactory foramen of *G. prasinus* lies on the posteroventral face of the basisphenoid (Fig. 1). In *A. allardicei*, it is the the pterosphenoid that ventrally bears a canal enclosing the olfactory nerve, with the olfactory foramensituated at the anterior face of the ptersphenoid (Fig. 2). The parasphenoid of both muraenids is a thick, long bone that forms the floor of the orbit (Figs.

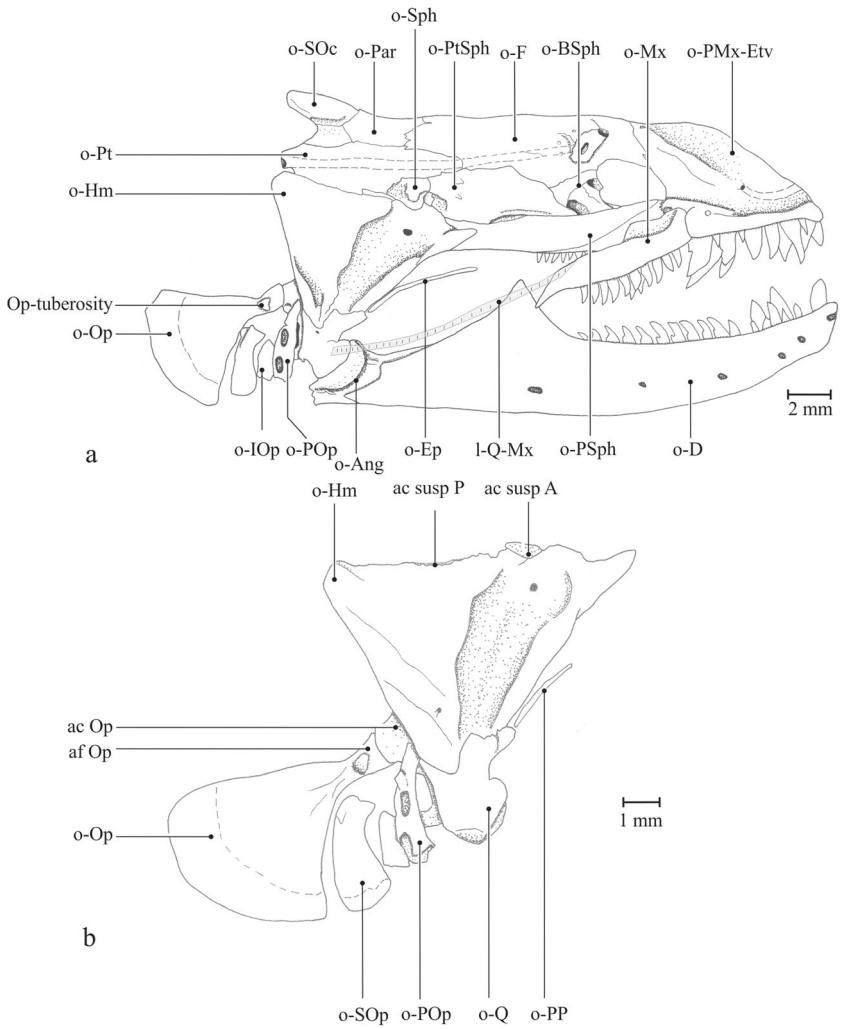

Fig. 1 Cranial skeleton of *Gymnothorax prasinus* (lateral view). **a** Skull (right side) and **b** suspensorium (right side). ac Op, opercular articular condyle; af Op, opercular articular facet; ac susp A, anterior suspensorial condyle; ac susp P, posterior suspensorial condyle; l-Q-Mx, quadrato-maxillary ligament; o-Ang, Angular bony complex; o-BSph, basisphenoid bone; o-D, dentary complex; o-ep, ectopterygoid; o-F, frontal bone; o-Hm, hyomandibular bone; o-Iop, interopercle; o-Mx, maxillary bone; o-Op, opercle; o-Par, parietal bone; o-PMx-Etv, premaxillo-ethmovomeral complex; o-POp, preopercle; o-PSph, parasphenoid; o-Pt, pterotic bone; o-PtSph, pterosphenoid bone; o-Q, quadrate; o-SOp, subopercle; o-Soc, supraoccipital bone; o-Sph, sphenotic bone; Op-tuberosity, opercular tuberosity

1a, 2a, 3b and 4b). It laterally expands in the mid-section and tapers posteriorly to a narrow process wedged into the basisphenoid (Figs. 3b and 4b).

The otic region of *G. prasinus* and *A. allardicei* comprise the sphenotics, pterotics, prootics, epioccipitals and parietals. The sphenotic of *G. prasinus* bears a lateral process directing ventrally, whereas that of *A. allardicei* is directed anteroventrally (Fig. 2a). In both muraenids, the pterotic forms the posterolateral element of the neurocranium and also the long posterior suspensorial articulatory facet (Figs. 3b and 4b). The prootic of *G. prasinus* is fenestrated with numerous foramina, including the trigemino-facial foramen on its anterolateral face (Fig. 3b). Its posterior end also bears an apophysis to which attaches the levator internus of the upper pharyngeal jaw (Fig. 5d). The lateroventral part of the prootic in *A. allardicei* bears a depression with three pores where the levator internus muscle inserts at the center of this depression (Fig. 4b). The trigemino-facial foramen of *A. allardicei* lies on the anterior rim of the prootic bone (Fig. 4b). The parietals of *G. prasinus* posteriorly border the epioccipital and supraoccipital bones, whereas in *A. allardicei*, they overlap with the epioccipitals. A fontanel is present at the triple suture point between the supraoccipital and parietals in *G. prasinus* (Fig. 3a). In both muraenids the posterior rim of the epioccipital is curved ventrally forming the dorsal rim of the posterior wall of the neurocranium.

In the occipital region, *G. prasinus* and *A. allardicei* have a supraoccipital that bears a well-developed crest directing caudally (Figs. 1a, 2a, 3a and 4a). The foramen magnum is bordered laterally by the exoccipitals and ventrally by the basioccipital. In both the exoccipital is domed towards the foramen magnum. Anteriorly, the basioccipital of *G. prasinus* bears two apophyses where the levator externus muscle of the upper pharyngeal jaws inserts onto. The posterior portion of the basioccipital in *G. prasinus* contributes to form a nipple-shaped, short otic bulla together with the exoccipital and prootic (Fig. 3b) and posteriorly, it bears four pores. In *A. allardicei*, the basioccipital also contributes to form the posterior part of the less protruding otic bullae along with the exoccipital and prootic (Fig. 4b).

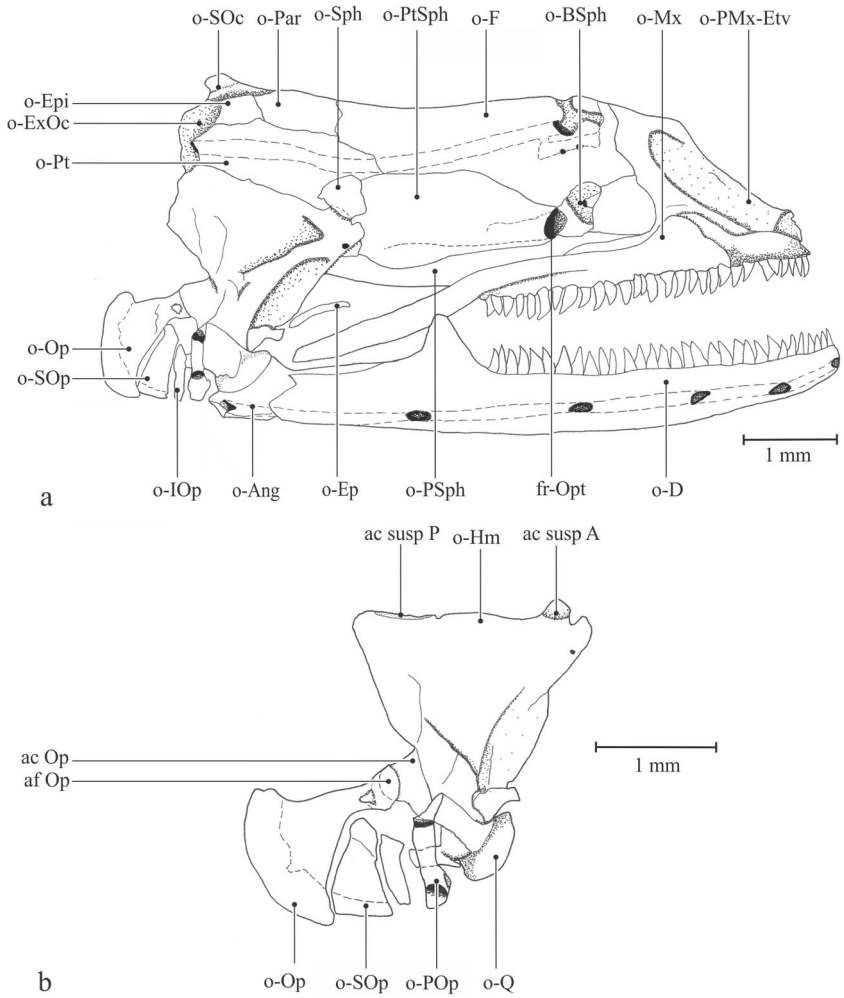

Fig. 2 Cranial skeleton of *Anarchias allardicei* (lateral view). **a** Skull (right side) and **b** suspensorium (right side). ac Op, opercular articular condyle; af Op, opercular articular facet; ac susp A, anterior suspensorial condyle; ac susp P, posterior suspensorial condyle; fr-Opt, foramen opticum; o-Ang, angular bony complex; o-BSph, basisphenoid bone; o-D, dentary complex; o-ep, ectopterygoid; o-ExOc, exoccipital bone; o-F, frontal bone; o-Hm, hyomandibular bone; o-Iop, interopercle; o-Mx, maxillary bone; o-Op, opercle; o-Par, parietal bone; o-PMx-Etv, premaxillo-ethmovomeral complex; o-POp, preopercle; o-PSph, parasphenoid; o-Pt, pterotic bone; o-PtSph, pterosphenoid bone; o-Q, quadrate; o-SOp, subopercle; o-Soc, supraoccipital bone; o-Sph, sphenotic bone

Jaws The maxillary of *G. prasinus* is attached to the strut of the posterodorsal process of the premaxillo-ethmovomeral complex. It bears two central rows of caniniform teeth on the anterior half with longer lateral ones, whereas posteriorly teeth are arranged in a single row (Fig. 6a). The maxillary of *A. allardicei* is longer than that of *G. prasinus* and attaches firmly to the maxillo-ethmovomeral articular facet of the premaxillo-ethmovomeral complex (Fig. 1a). In *A. allardicei*, the anterior part of the maxillary bears an ascending process that medially possesses two large teeth and also a single row of pointed teeth on its anteromedial fossa (Fig. 7a). The quadrato-maxillary ligament in *G. prasinus* connects the posterolateral face of the articulatory condyle of the quadrate to the posterodorsal face of the maxillary (Fig. 5a), whereas that of *A. allardicei* runs medial to the suspensorium and attaches to the medial face of the articulatory condyle of the quadrate.

In both muraenids, the large coronoid process is formed by the dentary complex. Anteriorly, the dentary complex of *G. prasinus* bears two rows of the caniniform teeth with three larger medial ones that continue in a single row of caudally pointed teeth running up to the coronoid process (Fig. 6b). The dentary in *A. allardicei* bears two rows of caniniform teeth, with a longer median row that runs up to the midpoint of the lateral one (Fig. 7b). Also, few small, recurved teeth are present medial to the longer ones (Fig. 7b). Lateraly, the dentary complex of *G. prasinus* bears six pores of the preoperculo-mandibular canal and one on its anteromedial face (Figs. 1a and 6b), whereas that of *A. allardicei* bears only five pores (Fig. 12a). The coronomeckelian bone in *G. prasinus* is situated between the dentary and angular complexes, ventral to the Meckelian fossa and anteriorly covered by the dentary (Fig. 6b). In *A. allardicei*, it is attached to the posteromedial face of the dentary and ventromedial face of the angular complex (Fig. 7b).

In both muraenids, the angular complex consists of the fused angular, articular and retroarticular bones. The mandibular articulation facet is positioned at the posterior end of this complex and is directed caudodorsally (Figs. 6b and 7b). The preoperculo-mandibular canal in both muraenids opens at the posterior side of the short, caudally directed retroarticular bone. In both muraenids, the anterolateral

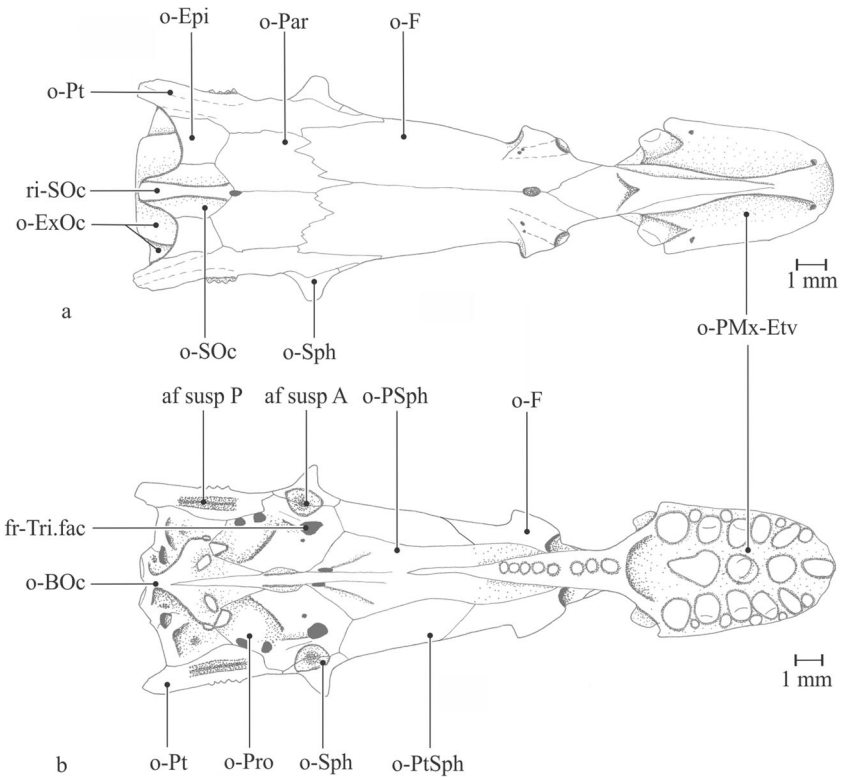

Fig. 3 Neurocranium of *Gymnothorax prasinus*. **a** Dorsal view and **b** ventral view. af susp A, anterior suspensorial articulation facet; af susp p, posterior suspensorial articulation facet; fr-Tri.fac, foramen trigemino-facialis; o-BOc, basioccipital bone; o-Epi, epioccipital bone; o-ExOc, exoccipital bone; o-F, frontal bone; o-Par, parietal bone; o-PMx-Etv, premaxillo-ethmovomeral complex; o-Pro, prootic bone; o-PSph, parasphenoid; o-Pt, pterotic bone; o-PtSph, pterosphenoid; o-Soc, supraoccipital bone; o-Sph, sphenotic bone; ri-Soc, supraoccipital crest

portion of the angular complex overlies the posterior part of the dentary complex. In *G. prasinus* and *A. allardicei*, a short preoperclo-angular ligament connects the posteromedial face of the angular complex to the ventro-medial face of the preopercle.

Suspensorium and opercular series In both muraenids, the suspensorium comprises four bones including the ectopterygoid, quadrate, hyomandibula and preopercle (Figs. 1b and 2b). The ectopterygoid is reduced, forming a thin, slender bone attaching to the anteroventral edge of

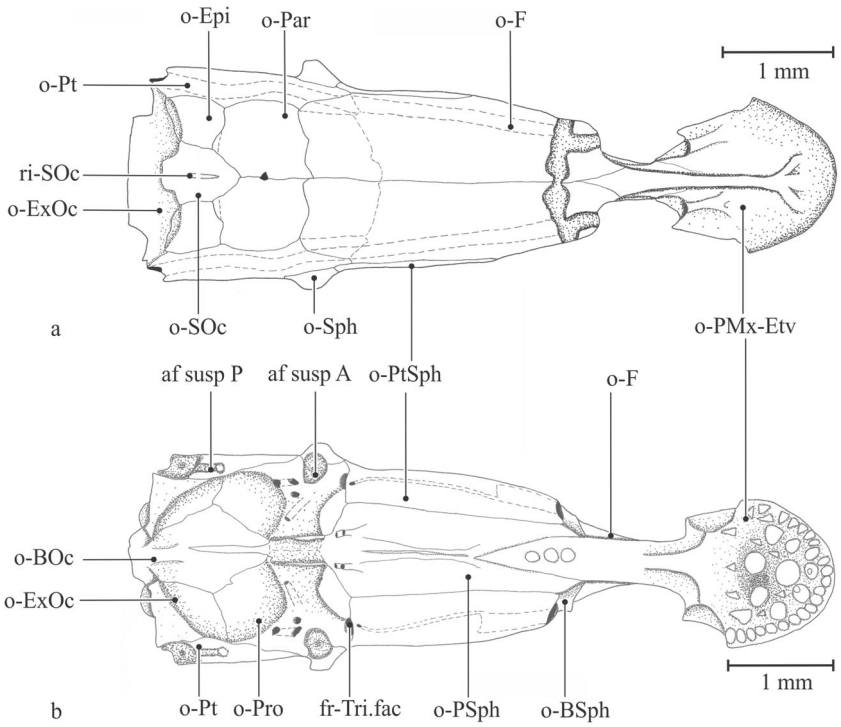

Fig. 4 Neurocranium of *Anarchias allardicei*. **a** Dorsal view and **b** ventral view. af susp A, anterior suspensorial articulation facet; af susp p, posterior suspensorial articulation facet; fr-Tri.fac, foramen trigemino-facialis; o-BOc, basioccipital bone; o-BSph, basisphenoid; o-Epi, epioccipital bone; o-ExOc, exoccipital bone; o-F, frontal bone; o-Par, parietal bone; o-PMx-Etv, premaxillo-ethmovomeral complex; o-Pro, prootic bone; o-PSph, parasphenoid; o-Pt, pterotic bone; o-PtSph, pterosphenoid; o-Soc, supraoccipital bone; o-Sph, sphenotic bone; ri-Soc, supraoccipital crest

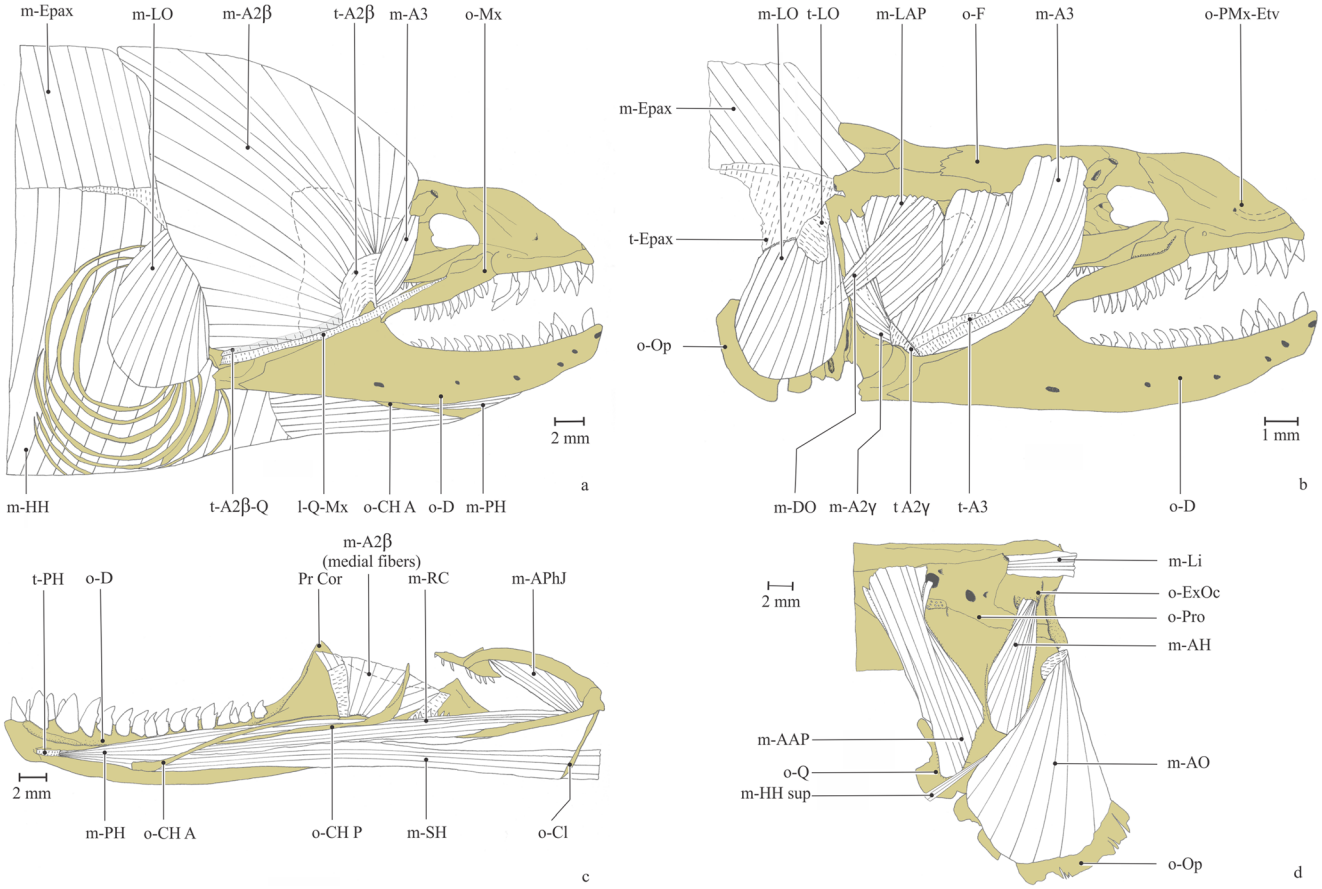

Fig. 5 The cranial muscles of *Gymnothorax prasinus*. **a** Skin removed (lateral view), **b** sections A2, hyohyoideus muscle complex, hypaxial muscles, ventral elements of the head and quadrate-maxillary ligament and branchiostegal rays are removed (lateral view) and **c** ventral muscles of head (sagittal left cut), hyohyoideus muscle complex is removed. l-Q-Mx, quadrato-maxillary ligament; m-A2β, lateral subsection of A2β; m-A2γ, medial subsection of A2; m-A3, A3 section of the adductor mandibulae muscle complex; m-AAP, adductor arcus palatini muscle; m-AH, adductor hyomandibulae muscle; m-AO, adductor operculi muscle; m-APhJ, adductor muscle of the pharyngeal jaw; m-DO, dilatator operculi muscle; m-Epax, epaxial muscles; m-HH, hyohyoideus muscle complex; m-HH sup, hyohyoideus superior muscle; m-LAP, levator arcus palatini muscle; m-Li, levator internus muscle; m-LO, levator operculi muscle; m-PH, protractor hyoidei muscle; m-RC, rectus communis muscle; m-SH, sternohyoideus muscle; o-CH A, anterior ceratohyal bone; o-CH P, posterior ceratohyal bone; o-Cl, cleithrum; o-D, dentary complex; o-ExOc, exoccipital bone; o-F, frontal bone; o-Mx, maxillary bone; o-Op, opercle; o-PMx-Etv, premaxillo-ethmovomeral complex; o-Pro, prootic bone; o-Q, quadrate bone; t-A2β, tendon of A2β; t-A2β-Q, A2-quadrate tendon; t-A2γ, tendon of A2γ; t-A3, tendon of A3; t-Epax, tendon of epaxial muscles; t-LO, tendon of levator operculi; t-PH, tendon of protractor hyoidei; pr Cor, coronoid process

the hyomandibula by connective tissue and ligamentously on the anterior end of the quadrate. The quadrate bears a posterior, caudally directed process that runs medial to the preopercle. The hyomandibula-quadrate axis is directed vertically, thus positioning the quadrate-mandibular joint at the occipital level of the neurocranium and explaining the lower jaw being about equal in length to the neurocranium. Anteriorly, the hyomandibula bears a fossa with a pore on its dorsal half (Figs. 1b and 2b). Medially, it bears a canal that is opened on its dorsomedial face. The posterior articular condyle of the hyomandibula is long with serrated edges on its dorsal midsection. The triangular hyomandibula medioventrally bears an opercular articulatory condyle that is directed caudoventrally (Figs. 1b and 2b).

In *G. prasinus*, the four elements of the opercular series are reduced in size (Fig. 1b). The preopercle is a small, tube-like bone connected to the quadrate. It encloses the midsection of the preoperculo-mandibular canal. The opercle bears an anterolateral tuberosity on its articulatory process (Fig. 1b) that also bears a small process on the medial face. The small rectangular subopercle and interopercle lie in between the opercle and the preopercle (Fig. 1b). A similar opercular series is found in *A. allardicei*, except for the absence of a middle pore on the lateral face of the preopercle (Fig. 2b).

Hyoid complex The hyoid complex of *G. prasinus* is extremely reduced and consists of the paired anterior and posterior ceratohyals (Fig. 5c). The anterior and posterior ceratohyals are slender bones interconnected by a synchondrosis. The

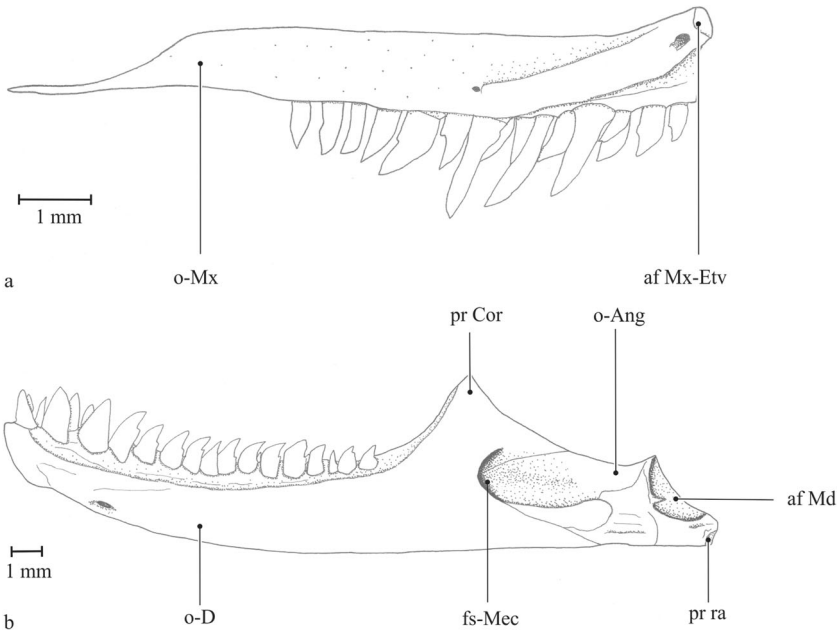

Fig. 6 Jaws of *Gymnothorax prasinus* (right side) **a** maxillary; lateral view and **b** lower jaw; medial view. af Md, mandibular articulation facet; af Mx-Etv, maxillo-ethmovomeral articular facet; o-Ang, angular bony complex; o-D, dentary complex; o-Mx, maxillary bone; fs-Mec, meckelian fossa; pr Cor, coronoid process; pr ra, retroarticular process

posterior ceratohyal is connected to all eight branchiostegal rays anteriorly and to the medial face of a posterior process of the quadrate by connective tissue. The hyoid complex of *A. allardicei* is also extremely reduced, showing a simular morphology as in *G. prasinus* with less branchiostegal rays (5 ver. 7 of *A. allardicei*) (Fig. 8c).

Lateral line system The cephalic lateral line system of *G. prasinus* comprises the ethmoid, supraorbital, infraorbital, adnasal, temporal and preoperculo-mandibular canals, and supratemporal commissure (Fig. 9b). The ethmoid canal is a short descending branch of the supraorbital canal and starts at the anterior edge of the olfactory cavity. It bears a single external pore. The supraorbital canal is caudally extended to the dorsal pore of the anterolateral process of the frontal. Anteriorly, it is enclosed by a tube-like nasal bone and posteriorly by two supraorbital bones (Fig. 9a). The supraorbital canal bears one external pore. The infraorbital canal is curved dorsally into the postorbital region after exiting the first infraorbital bone positioned ventral to the orbit (Fig. 9a). This canal anstomoses with the supraorbital canal inside the anterolateral process of the frontal. The infraorbital canal bears four external pores. Anteriorly, the infraorbital canal is supported by the lacrimal and first infraorbital bones and posteriorly, by three infraorbital bones (Fig. 9a). The adnasal canal is an ascending branch of the infraorbital canal exited from the medial face of the ventral infraorbital bone at its midpoint.

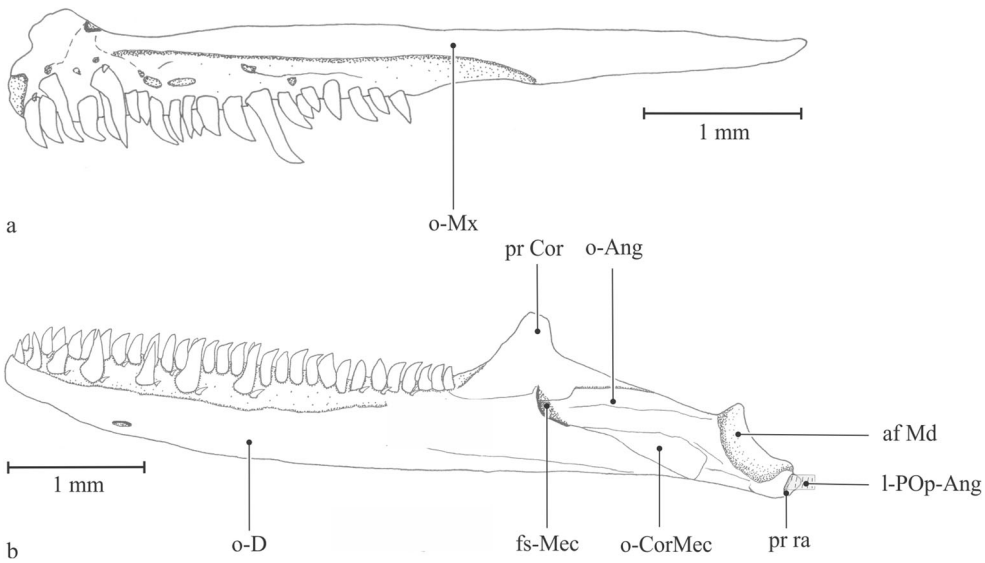

Fig. 7 Jaws of *Anarchias allardicei* (right side). **a** maxillary; medial view and **b** lower jaw; medial view. af Md, mandibular articulation facet; l-Pop-Ang, preoperculo-angular ligament; o-Ang, angular bony complex; o-D, dentary complex; o-CorMec, coronomeckelian bone; o-Mx, maxillary bone; fs-Mec, meckelian fossa; pr Cor, coronoid process; pr ra, retroarticular process

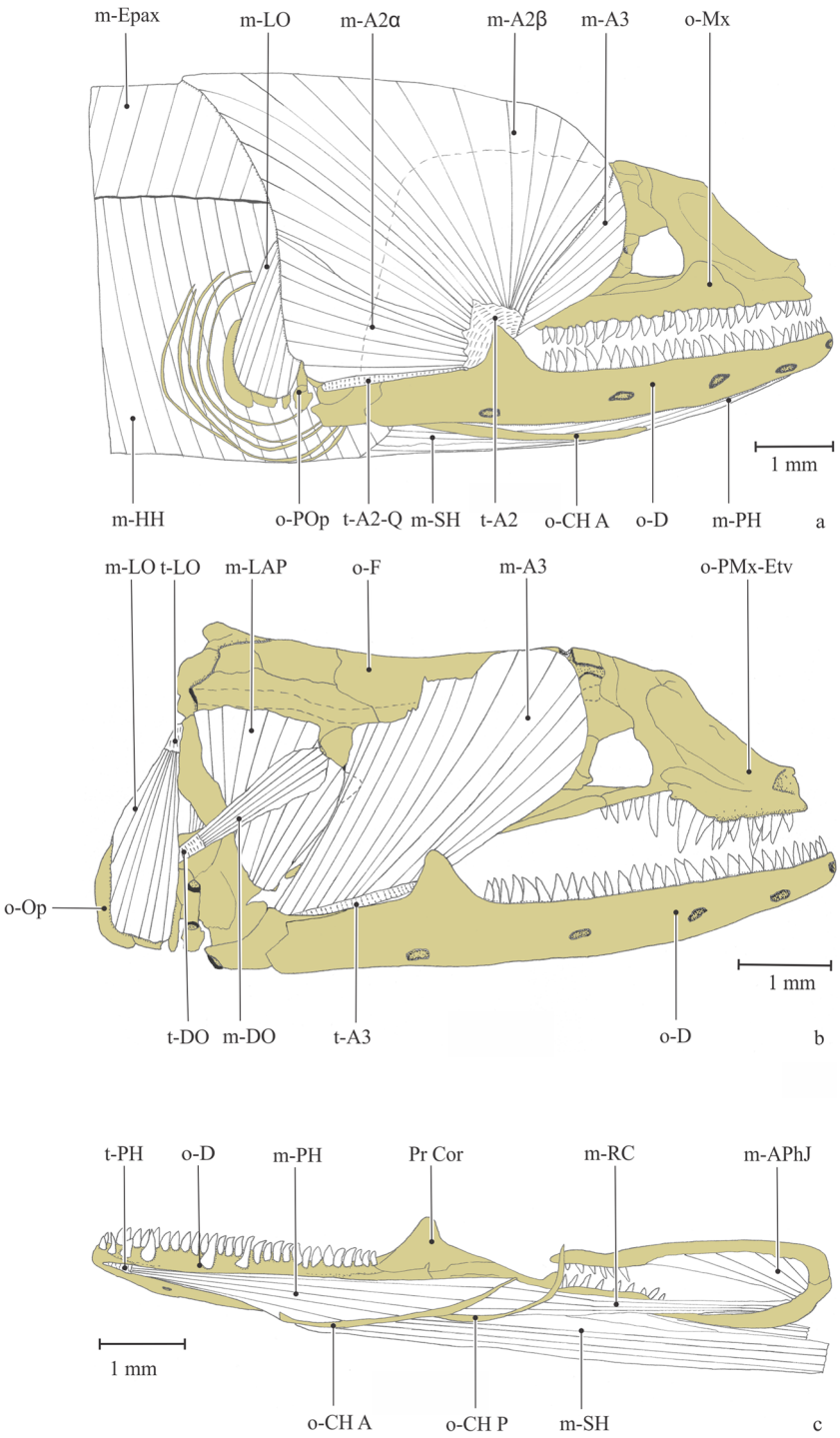

Fig. 8 The cranial muscles of *Anarchias allardicei*. **a** Skin removed (lateral view), **b** sections A2, hyohyoideus muscle complex, epaxial muscles, hypaxial muscles, ventral elements of the head and quadrato-maxillary ligament and branchiostegal rays are removed (lateral view) and **c** ventral muscles of head (sagittal left cut) and position of the pharyngeal jaws in relation to the lower jaw and hyoid apparatus, hyohyoideus muscle complex is removed. m-A2α, ventral subsection of A2; m-A2β, dorsal subsection of A2; m-A3, A3 section of the adductor mandibulae muscle complex; m-APhJ, adductor muscle of the pharyngeal jaw; m-DO, dilatator operculi muscle; m-Epax, epaxial muscles; m-HH, hyohyoideus muscle complex; m-LAP, levator arcus palatini muscle; m-LO, levator operculi muscle; m-PH, protractor hyoidei muscle; m-RC, rectus communis muscle; m-SH, sternohyoideus muscle; o-CH A, anterior ceratohyal bone; o-CH P, posterior ceratohyal bone; o-D, dentary complex; o-F, frontal bone; o-Mx, maxillary bone; o-Op, opercle; o-PMx-Etv, premaxillo-ethmovomeral complex; o-POp, preopercle; t-A2, tendon of A2; t-A2-Q, A2-quadrate tendon; t-A3, tendon of A3; t-DO, tendon of dilatator operculi muscle; t-LO, tendon of levator operculi; t-PH, tendon of protractor hyoidei; pr Cor, coronoid process

This canal is supported at its midpoint by the adnasal bone. All circumorbital bones are tubular (Fig. 9a). The preoperculo-mandibular canal runs inside the mandibula (Fig. 9b).

Compared to *G. prasinus*, the cephalic lateral line system of *A. allardicei* lacks the ethmoid and adnasal canals and possesses a frontal commissure (Fig. 10b). The posterior part of the supraorbital canal enters the frontal through the anterior part of the frontal groove. The supraorbital canal bears three external pores. The frontal commissure runs inside the dorsal part of the frontal groove (Fig. 10b). The infraorbital canal anstomoses with the supraorbital canal at the front of the frontal groove. This canal bears five external pores. A lacrimal and seven infraorbital bones support the infraorbital canal (Fig. 10a). The preoperculo-mandibular canal bears six external pores.

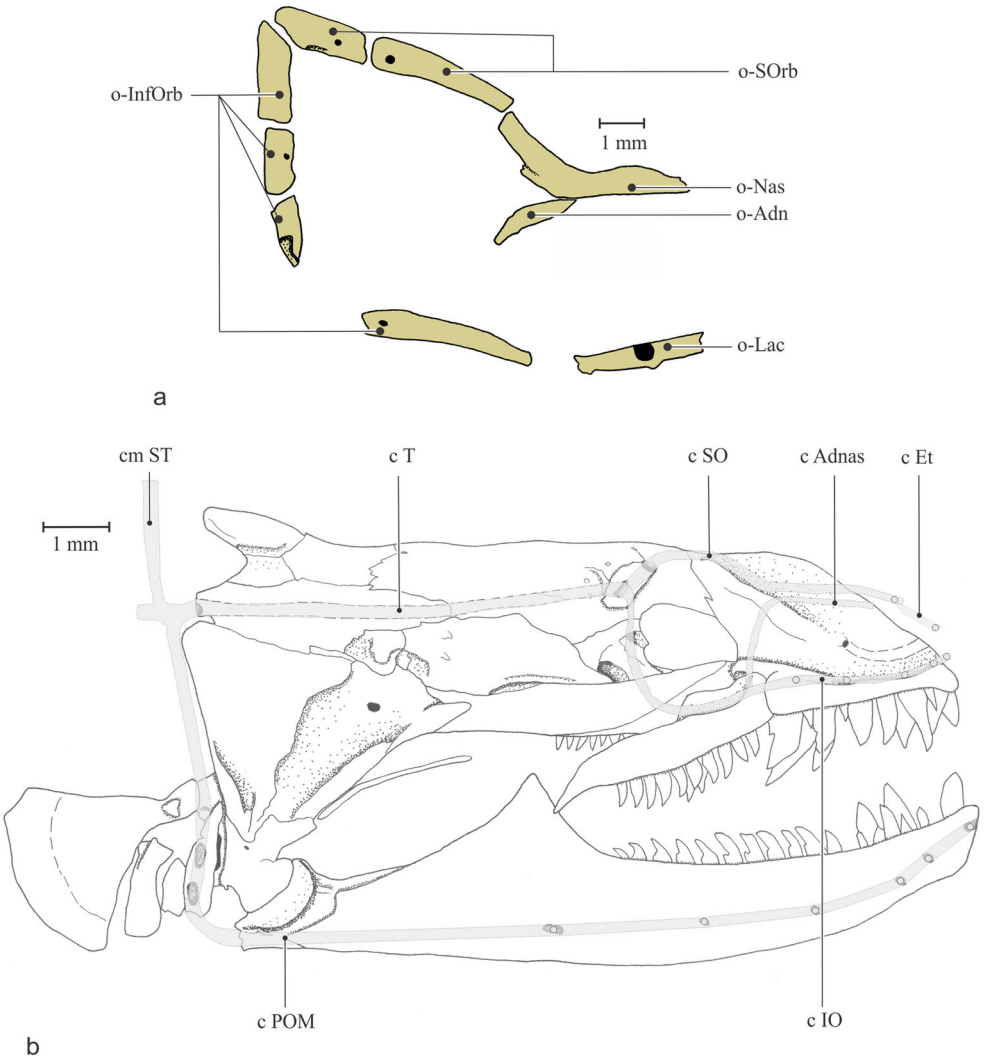

Fig. 9 The cranial lateral line system and circumorbital bones of *Gymnothorax prasinus*. **a** Lateral view of the nasal bone, preorbital bones, infraorbital bone, postorbital bones and supraorbital bones (right side) and **b** position of the composing canals in relation to the skull (right side, lateral view). c Adnas, adnasal canal; c Et, ethmoid canal; c IO, infraorbital canal; c POM, preopercular mandibular canal; c SO, supraorbital canal; c T, temporal canal; cm ST, supratemporal commissure; o-Nas, nasal bone; o-Adn, adnasal bone; o-InfOrb, infraorbital bone; o-Lac, lacrimal bone; o-SOrb, supraorbital bone

Gill arches In *G. prasinus*, the reduced gill arches comprise the following ventral elements: four pairs of ceratobranchials (Cb I-IV) and one pair of upper pharyngeal tooth plates (UP) (Fig. 11b). The dorsal elements comprised the four pairs of epibranchials (Eb I-IV) and one pair of lower pharyngeal tooth plates (LP) (Fig. 11a). The gill arches in *A. allardicei* bears two pairs of infrapharyngobranchials (Ib I-II) thas is absent in *G. prasinus* (Fig. 12).

Cranial myology

Adductor mandibulae complex The adductor mandibulae muscle complex is hypertrophied and similar in morphology in *G. prasinus* and *A. allardicei*, comprising the sections A2 and A3. In *G. prasinus,* A2 is subdivided into a hypertrophied lateral (A2β) and medial (A2γ) parts (Fig. 5a, b). A2β forms the largest element of the adductor mandibulae complex, with its fibers originating from the frontal, parietal, pterotic, supraoccipital, hyomandibula and quadrate bones. The antero-lateral fibers of A2β insert as a tendon on the medial face of the dentary at the rear of the coronoid process, whereas its posterolateral fibers are attached as a separate tendon on the mediodorsal edge of the coronoid process and medial margin of the angular bone. Also, the latter tendon is connected to the lateral face of the articulatory condyle of the quadrate. The medial fibers of A2β insert musculously into the Meckelian fossa (Fig. 5c), whereas the A2γ is runs posteriorly to the levator arcus palatini and medially to the dilatator operculi muscle (Fig. 5b). The fibers of A2γ originate from the posterodorsal face of the hyomandibula and insert by a tendon on the angular complex, at the ventral rim of the Meckelian fossa (Fig. 5b). In *A. allardicei,* A2 comprises next to the dorsally positioned A2β part also a ventral A2α part (Fig. 8a). The A2β is the largest component and its fibers originate from the frontal, parietal, pterotic, epioccipital and supraoccipital bones. This muscle inserts as a tendon on the ventromedial face of the coronoid process and musculously on the medial rim of the dentary and angular, posterior to the coronoid process. The A2α of *A. allardicei* is the ventral element and has a muscle origin at the posterior part of the

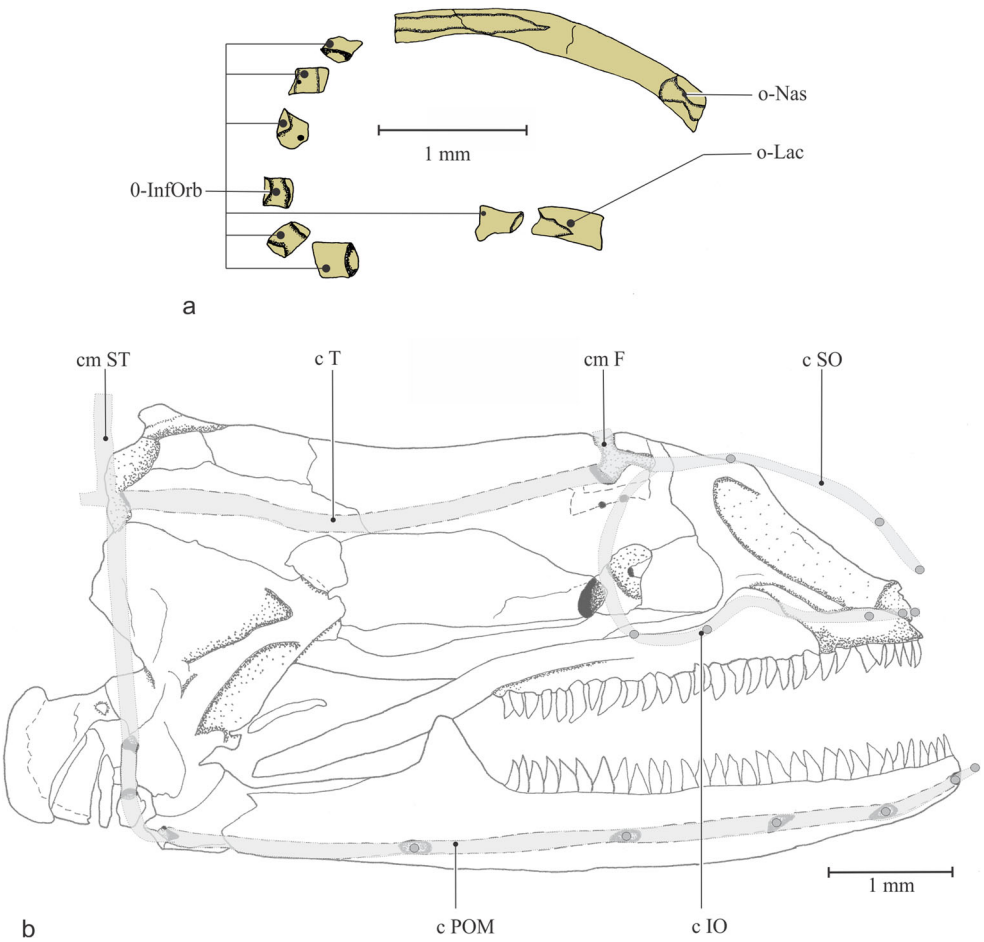

Fig. 10 The cranial lateral line system and circumorbital bones of *Anarchias allardicei*. **a** lateral view of the nasal bone, preorbital bones and postorbital bones (right side) and **b** position of the composing canals in relation to the skull (right side, lateral view). c IO, infraorbital canal; c POM, preopercular mandibular canal; c SO, supraorbital canal; c T, temporal canal; cm F, frontal commissure; cm ST, supratemporal commissure; o-Nas, nasal bone; o-InfOrb, infraorbital bone; o-Lac, lacrimal bone

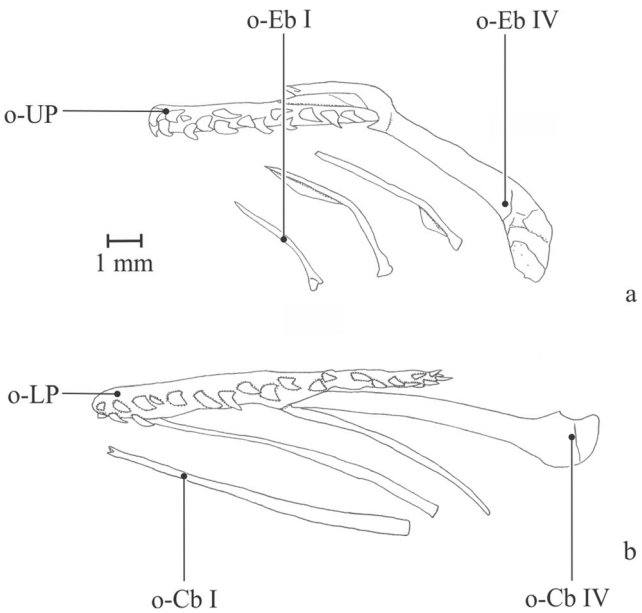

Fig. 11 Gill arches of *Gymnothorax prasinus*. **a** Ventral view of the dorsal elements and **b** dorsal view of the ventral elements. o-Cb, ceratobranchial bone; o-Eb, epibranchial bone; o-LP, lower pharyngeal tooth plates; o-UP, upper pharyngeal tooth plates

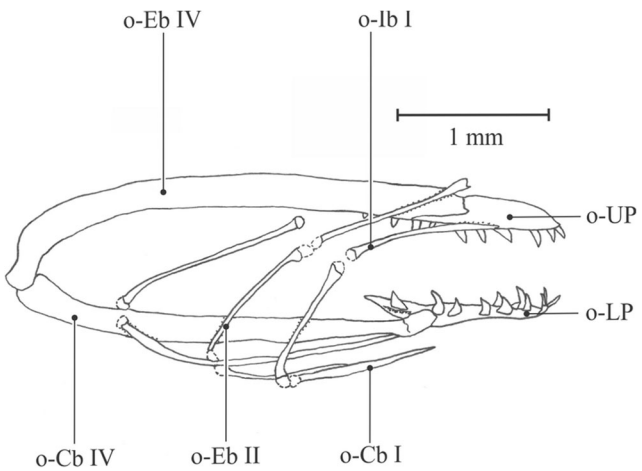

Fig. 12 Gill arches of *Anarchias allardicei*. Lateral view of the ventral and dorsal part of the gill arches (right side). o-Cb, ceratobranchial bone; o-Eb, epibranchial bone; o-Ib, infrapharyngobranchial bone; o-LP, lower pharyngeal tooth plates; o-UP, upper pharyngeal tooth plates

hyomandibula and quadrate bones (Fig. 8a). The medial fibers of A2α insert musculously into the Meckelian fossa and its lateral fibers attach both tendinously and musculously on the posteromedial face of the angular complex. In both muraenids the posterolateral fibers of the left and right A2β subsection merge with their counterparts fibers and are also connected tendinously to the epaxial muscles and a fascia seperating them from the levator operculi muscle (Figs. 5a and 8a).

The A3 section is a large muscle with its anterior fibers directing caudoventrally in both *A. allardicei* and *G. prasinus* (Figs. 5b and 8b). In *G. prasinus*, it originates musculously from the frontal, pterosphenoid, pterotic, posterior part of the basisphenoid, parasphenoid and anterolateral face of the sphenotic bones (Fig. 5b). Its anterior fibers are connected to the ventromedial face of the angular complex through a tendon, whereas its posterior fibers attach musculously to its posteromedial face. In *A. allardicei*, A3 fibers originate musculously from the frontal, pterosphenoid, posterior part of the basisphenoid and anterolateral face of the sphenotic bones (Fig. 8b). Its anterior fibers insert through a tendon into the posterior part of the Meckelian fossa and its posterior fibers attach musculously on the posterodorsal margin of the medial face of the angular complex.

Suspensorial muscles The morphology of the suspensorial muscles is very similar for both *G. prasinus* and *A.allardicei*. The adductor arcus palatini originates musculously from the depression of the prootic at the rear of the trigemino-facial foramen and inserts on the anteromedial face of the hyomandibula and dorsomedial face of the quadrate (Fig. 5d).

The levator arcus palatini is positioned posterior to the A3 section of the adductor mandibulae complex, by which it is also covered anterodorsally (Figs. 5b and 8b). The fibers originate from the ventral and medial faces of the sphenotic process and lateroventral face of the pterotic. This muscle inserts on the posterior face of the hyomandibula and anterodorsal margin of the quadrate (Figs. 5b and 8b). The adductor hyomandibulae muscle connects the posteroventral margin of the medial face of the hyomandibula to a depression on the posterolateral face of the exoccipital (Fig. 5d).

Opercular muscles The dilatator operculi is a caudoventrally directed muscle strip in both *G. prasinus* and *A. allardicei* (Figs. 5b and 8b). In *G. prasinus*, it originates musculously from the lateral face of the sphenotic process and ventrolateal face of the pterotic and inserts on the process of the medial face of the opercular rostral prominence (Figs. 5b and 8b). In *A. allardicei*, it originates musculously only from the lateral face of the sphenotic process and inserts through a tendon onto the anteromedial face of the opercular rostral prominence (Fig. 8b).

In *G. prasinus*, the anterior fibers of the levator operculi originate through a tendon from the posterodorsal edge of the hyomandibula, whereas the posterior fibers originate from a tendon that attsches to the epaxial muscles and anterior part of the horizontal septum between the epaxial and hypaxial muscles (Fig. 5d). In *A. allardicei*, all fibers originate through a tendon from the posterodorsal edge of the hyomandibula (Fig. 8b). In both species, the muscle inserts on the lateral faces of the opercle, subopercle and interopercle (Figs. 5b and 8b).

The adductor operculi muscle originates in both *G. prasinus* and *A. allardicei* as a tendon from the dorsomedial corner of the hyomandibula and inserts on the medial faces of the opercle, subopercle and interopercle (Fig. 5d). In *G. prasinus*, the adductor operculi tendon is also connected to the tendon of the epaxial muscles.

Hyoid muscles The protractor hyoidei muscle connects the long, thin and flexible anterior ceratohyal bone to the lower jaw in both *G. prasinus* and *A. allardicei*. It originates tendinously from the medial face of the dentary bone, close to the symphysis, and inserts musculously on the anterior face of the anterior ceratohyal (Figs. 5c and 8c).

The sternohyoideus in *G. prasinus* and *A. allardicei* originates anteriorly from the anterior half of the anterior ceratohyal, attaching to a myoseptum connecting it to the hypaxial muscles (Figs. 5c and 8c). The hyohyoideus superior in *G. prasinus* connects the posterior end of the posterior ceratohyal to a small process on the medial face of the opercular rostral prominence (Fig. 5d). This muscle is absent in *A. allardicei.* The hyohyoideus muscle complex in *G. prasinus* and *A. allardicei* is a muscle sheet that lies between the medial faces of the branchiostegal rays and forms a thin sac-like muscle meeting its counterpart at the ventral midline (Figs. 5a and 8a). The dorsal fibers attach to the horizontal septum between the epaxial and hypaxial muscles.

Body musculature The epaxial muscles in *G. prasinus* and *A. allardicei* insert musculously on the epioccipital, supraoccipital, exoccipital and basioccipital bones. As mentioned, the hypaxial muscles attach directly to the sternohyoideus muscle through a myoseptum.

Branchial muscles In both muraenids, the rectus communis muscle originate from the posterior half of the anterior ceratohyal and attaches to the fourth ceratobranchial bone (Figs. 5c and 8c).

The fibers of the levator externus and levator internus in *G. prasinus* insert on the basioccipital and prootic bones, respectively. Those of *A. allardicei* are attached to the exoccipital and the prootic, respectively. Other muscles serving the branchial arches of *G. prasinus* and *A. allardicei* are similar to those described in Mehta and Wainwright (2007a).

Discussion

Morays are carnivores and shallow-water reef, crevice-dwelling eels that are found in all tropical and subtropical oceans and seas, with a few species occurring in temperate waters (Böhlke et al. 1989; Santos and Castro 2003; Young and Winn 2003). Morays like many fish swallow their large prey as a whole, with for example gulper eels having extensive jaw and skin modifications to engulf larger prey items (Yukihira et al. 1994; Santos and Castro 2003; Westneat 2007). Morays have evolved an alternative prey transport to move large prey from the oral jaws to the pharyngeal jaws, different from hydraulics based system observed in most fishes and even most Anguilliformes (Mehta and Wainwright 2007a, 2008) such as *A. gilberti* (Eagderi and Adriaens 2014). Compared to these Anguilliformes that perform hydraulics based prey transport, including the closely-related *A. gilberti* (Eagderi and Adriaens 2014), some cephalic features of muraenids can be considerd as specializations to seize and devoure large prey relying on this second set of jaws.

The neurocranial elements of muraenids, such as the premaxillo-ethmovomeral complex and parasphenoid are stout and robust, compared to that of *A. gilberti* (Eagderi and Adriaens 2014). Considering also the hypertrophied nature of the jaw adductor muscles in muraenids (inserting on a supraoccipital crest), as well as their jaws (dentary, premaxillary and maxillary) and teeth being larger and more robust, these reinforcements may help in resisting high levels of mechanical stress during biting and prey grabbing (Grubich et al. 2008). In moray eels, almost the full anterior half of the dentary complex of muraenids is dentigerous with larger anterior teeth, and teeth on the maxillary and premaxillo-ethmovomeral complex are extended caudally. As shown by Mehta and Wainwright (2007b), muraenids impale large prey with the anterior part of oral jaw, where prey can be restrained efficiently as teeth sink into the prey.

The posterior position of the quadrato-mandibular articulation in the muraenids, being approximately at the level of the posterior margin of the neurocranium, is associated with the elongation of the lower jaw and a large, non-circular gape in muraenids. An aquatic predator with such a gape morphology can move the jaws into a biting position), as well as consuming large preys (Castle 1968; Porter and Motta 2004; Mehta and Wainwright 2007a, 2008; Mehta 2009). In other Anguilliformes, such as Nemichthyidae, Nettastomidae and Serrivomeridae, jaw elongation is associated with an elongation of the rostral region, rather than with a caudally tilted suspensorium (Smith and Nielsen 1989; Tighe 1989; Eagderi and Adriaens 2010a). Long lower jaws are known to facilitate fast mouth closure, effective for capturing mobile and elusive prey, as observed in these muraenids (Lauder 1979; Norton and Brainerd 1993; Westneat 2004; Porter and Motta 2004; Eagderi and Adriaens 2010a). For instance, mechanical advantage for opening and closing of the lower jaw in *Gymnothorax javanicus* (Bleeker, 1859) is low, implying the jaws to be kinematically efficient for fast biting (Westneat 2004).

It has been suggested that species with enlarged jaw adductors appear "adapted" to feed at higher gape angles (Gans and De Vree 1987), although this probably is not the case for muraenids. Morays are well suited for closing the tips of the jaws at high velocities but consequently have a mechanical disadvantage for force production at their jaw tips (Porter and Motta 2004). Increasing of force and velocity transfer in mouth closing systems, as trade-offs, have been suggested before in fish species (Westneat 1994, 2004; Turingan et al. 1995; Collar et al. 2005; Kammerer et al. 2005; Van Wassenbergh et al. 2005; De Schepper et al. 2008). Morays, therefore may compensate for the mechanical disadvantage of force transmission through an increased input contraction force of their hypertrophied jaw-closing muscles, that allows fast ánd powerful impaling of prey using their sharp teeth (Devaere et al. 2001; Herrel et al. 2002; Van Wassenbergh et al. 2004). This allows an efficient immobilization of large prey, for the pharyngeal jaws to be protracted to deliver a second bite and subsequent prey transport (Mehta and Wainwright 2007b).

A mechanical bottle-neck in the powerful oral jaw system in muraenids, however, seems to be the presence of a highly reduced bony connection between the quadrate and the neurocranium (only splint-like ectopterygoid present). In teleosts, this rostral arm of the suspensorium generally forms a fortifying strut connecting the suspensorium to the rostral part of the neurocranium (Schaeffer and Rosen 1961). Ancestral for Anguilliformes is a slender ectopterygoid, wedging around the anterior part of the quadrate but lacking a strong articulatory connection with the neurocranium (Johnson et al. 2012). In other taxa, the ectopterygoid is well-developed (such as in *Hoplunnis* and *Conger*) or shows various degrees of reductions (e.g. slender bone contacting the neurocranium in *Anguilla* up to a splint-like bone not reaching the neurocranium, as observed in *Moringua* and the muraenids studied here) (De Schepper et al. 2005; Eagderi 2010; Johnson et al. 2012). In both clades having this anterior decoupling of the quadrate from the neurocranium (*Moringua* and muraenids), the fibers of the A3 part of the adductor mandibulae complex run from a dorsorostral to a ventrocaudal direction, hence generating a torque force onto the suspensorium that would pull the quadrate forward (this is not the case in species like *A. gilberti*). It is thus surprising that in those species that also show extensive jaw muscle hypertrophy, this bony strut that could prevent this, is missing. However, as discussed by De Schepper et al. (2005), counteracting force components of other muscle parts of the jaw adductor may reduce this forward pulling. Similar forces acting upon the quadrate-mandibular joint can then assist on stabilizing that joint as well. In muraenids, some additional fortifications of this joint involved the presence of quadrato-maxillary and preoperclo-angular ligaments and the

connection of the quadrate to the A2 tendon of adductor mandibulae complex. Whereas in taxa like *Moringua* and *Pythonichthys*, this may be linked to head-first burrowers (De Schepper et al. 2007; Eagderi and Adriaens 2010b), in muraenids it may play a more important role in keeping the jaws lodged when immobilizing large prey prior to grasping them with the pharyngeal jaws.

The observation that muraenids do not rely on a hydraulic, but rather pharyngeal jaw transport system for prey transport, is also reflected in the reduced nature of the opercular and the hyoid apparatus, as well as in the reduced number and size of the branchial arch elements (Mehta and Wainwright 2008). In doing so, these reductions did provide more room in the orobranchial cavity facilitating the mobility of the pharyngeal jaws.

An innovative pharyngeal jaw apparatus, as present in morays, enabled the use of a mechanical transport system rather than a hydraulic one to pull prey into the esophagus (Mehta and Wainwright 2007a). This study shows that this innovative feeding mechanism may be linked to many cephalic modifications, such as stout and robust neurocranial elements, elongated lower jaw as result of the posterior position of the quadrato-mandibular articulation, enlarged teeth of oral jaws and premaxillo-ethmovomeral complex, reduction in the moveable cranial bones and their muscular connections, hypertrophied adductor mandibulae muscle complex, presence of the quadrato-maxillary and preoperclo-angular ligaments, connection of the quadrate to the A2 tendon of adductor mandibulae complex and caudoventral orientation of the fibers of large A3 section of adductor mandibulae complex.

Acknowledgments The authors would like to thanks University of Tehran and Ghent University for financial support, M. McGrouther (Australian Museum) for providing museum specimens, and D.G. Smith (Smithsonian, USA) for his valuable comments.

Compliance with ethical standards

Conflict of interest The authors confirm that there are no known conflicts of interest associated with this publication.

References

Adriaens D, Verraes W, Taverne L (1997) The cranial lateral-line system in *Clarias gariepinus* (Burchell, 1822) (Siluroidei: Clariidae): morphology and development of canal related bones. Eur J Morphol 35(3):181–208

Bock WJ, Shear RC (1972) A staining method for gross dissection of vertebrate muscles. Anatomischer Anzeiger Bd 130:222–227

Böhlke EB (1989) Methods and terminology. In: Böhlke EB (ed) Fishes of the western North Atlantic. Sears Foundation for Marine Research, New Haven, pp 1–7

Böhlke EB, Mccosker JE, Böhlke JE (1989) Family Muranidae - morays. In: Böhlke EB (ed) Fishes of the western North Atlantic. Sears Foundation for Marine Research, New Haven, pp 104–206

Castle PHJ (1968) The world of eels. Tuatara: Journal of the Biological Society 16(2):87–97

Collar DC, Near TJ, Wainwright PC (2005) Comparative analysis of morphological diversity: does disparity accumulate at the same rate in two lineages of centrarchid fishes? Evolution 59:783–794. https://doi.org/10.1111/j.0014-3820.2005.tb01826.x

De Schepper N, Adriaens D, De Kegel B (2005) *Moringua edwardsi* (Moringuidae: Anguilliformes): cranial specialization for head-first burrowing? J Morphol 226:356–368

De Schepper N, De Kegel B, Adriaens D (2007) *Pisodonophis boro* (Ophichthidae: Anguilliformes): specialization for head-first and tail-first burrowing? J Morphol 268:112–126. https://doi.org/10.1002/jmor.10507

De Schepper N, Van Wassenbergh S, Adriaens D (2008) Morphology of the jaw system in trichiurids: trade-offs between mouth closing and biting performance. Zool J Linnean Soc 152:717–736. https://doi.org/10.1111/j.1096-3642.2008.00348.x

Devaere S, Adriaens D, Verraes W, Teugels GG (2001) Cranial morphology of the anguilliform clariid *Channallabes apus* (Günther, 1873) (Teleostei: Siluriformes): adaptations related to a powerful biting? Zool J Linnean Soc 255:235–250. https://doi.org/10.1017/S0952836901001303

Eagderi S (2010) Structural diversity in the cranial musculoskeletal system in Anguilliformes: an evolutionary-morphological study. PhD thesis. Ghent University, Ghent, Belgium

Eagderi S, Adriaens D (2010a) Head morphology of the duckbill eel, *Hoplunnis punctata* (Nettastomatidae: Anguilliformes): a case of jaw elongation. Zoology 113(3):148–157. https://doi.org/10.1016/j.zool.2009.09.004

Eagderi S, Adriaens D (2010b) Cephalic morphology of *Pythonichthys macrurus* (Heterenchelyidae: Anguilliformes): specializations for head-first burrowing. J Morphol 271:1053–1065. https://doi.org/10.1002/jmor.10852

Eagderi S, Adriaens D (2014) Cephalic morphology of *Ariosoma gilberti* (Bathymyrinae: Congridae). Iranian Journal of Ichthyology 1(1):39–50

Gans C, De Vree F (1987) Functional bases of fiber length and angulation in muscle. J Morphol 192:63–85. https://doi.org/10.1002/jmor.1051920106

Gillis GB, Lauder GV (1995) Kinematics of feeding in bluegill sunfish: is there a general distinction between aquatic capture and transport behaviors? J Exp Biol 198:709–720

Grubich J, Rice AN, Westneat MW (2008) Functional morphology of bite mechanics in the great barracuda (*Sphyraena barracuda*). Zoology 111:16–29. https://doi.org/10.1016/j.zool.2007.05.003

Hanken J, Wassersug R (1981) The visible skeleton. A new double-stain technique reveals the nature of the "hard" tissues. Functional Photography 16:22–26

Herrel A, Adriaens D, Verraes W, Aerts P (2002) Bite performance in clariid fishes with hypertrophied jaw adductors as deduced by bite modeling. J Morphol 253:196–205. https://doi.org/10.1002/jmor.1121

Hildebrand M (1995) Analysis of vertebrate structure. 4th edn. Wiley, New York

Johnson GD, Ida H, Sakaue J, Sado T, Asahida T, Miya M (2012) A 'living fossil' eel (Anguilliformes: Protanguillidae, fam. Nov.) from an undersea cave in Palau. Proceedings of the Royal Society B-Biological Sciences 279(1730):934–943

Kammerer CF, Grande L, Westneat MW (2005) Comparative and developmental functional morphology of the jaws of living and fossil gars (Actinopterygii: Lepisosteidae). J Morphol 267:1017–1031. https://doi.org/10.1002/jmor.10293

Lauder GV (1979) Feeding mechanisms in primitive teleosts and in the halecomorph fish *Amia calva*. J Zool 187:543–578. https://doi.org/10.1111/j.1469-7998.1979.tb03386.x

Lopez JA, Westneat MW, Hanel R (2007) The phylogenetic affinities of the mysterious anguilliform genera *Coloconger* and *Thalassenchelys* as supported by mtDNA sequences. Copeia 2007 (4):959–966

Mehta RS (2009) Ecomorphology of the moray bite: relationship between dietary extremes and morphological diversity. Physiol Biochem Zool 82(1):90–103. https://doi.org/10.1086/594381

Mehta RS, Wainwright PC (2007a) Raptorial jaws in the throat help moray eels swallow large prey. Nature 449(6):79–82. https://doi.org/10.1038/nature06062

Mehta RS, Wainwright PC (2007b) Biting releases constraints on moray eel feeding kinematics. J Exp Biol 210:495–504. https://doi.org/10.1242/jeb.02663

Mehta R, Wainwright PC (2008) Functional morphology of the pharyngeal jaw apparatus in moray eels. J Morphol 269:604–619. https://doi.org/10.1002/jmor.10612

Nelson GJ (1966) Gill arches of teleostean fishes of the order Anguilliformes. Pac Sci 20(4):391–408

Nelson JS, Grande TC, Mark VH, Wilson MVH (2016) Fishes of the world. 4th edn. Wiley, INC

Norton SF, Brainerd EL (1993) Convergence in the feeding mechanics of ecomorphologically similar species in the Centrarchidae and Cichlidae. J Exp Biol 176:11–29

Obermiller LE, Pfeiler E (2003) Phylogenetic relationships of elopomorph fishes inferred from mitochondrial ribosomal DNA sequences. Mol Phylogenet Evol 26:202–214

Patterson C (1975) The braincase of pholidophorid and leptolepid fishes, with a review of the actinopterygian braincase. Philosophical Transactions of the Royal Society B: Biological Sciences 269: 275–579

Porter HT, Motta PJ (2004) A comparison of strike and prey capture kinematics of three species of piscivorous fishes: Florida gar (*Lepisosteus platyrhinchus*), redfin needlefish (*Strongylura notata*), and great barracuda (*Sphyraena barracuda*). Mar Biol 145:989–1000

Rojo AL (1991) Dictionary of evolutionary of fish osteology. CRC Press, Florida

Santos FB, Castro RMC (2003) Activity, habitat utilization, feeding behavior, and diet of the sand moray *Gymnothorax ocellatus* (Anguilliformes, Muraenidae) in the south western Atlantic. Biota Neatropica 3:1–7

Schaeffer B, Rosen DE (1961) Major adaptive levels in the evolution of the Actinopterygian feeding mechanism. Am Zool 1(2):187–204

Smith DG, Nielsen JG (1989) Family nemichthyidae. In: Böhlke EB (ed) Fishes of the western North Atlantic. Sears Foundation for Marine Research, New Haven, pp 411–459

Tighe KA (1989) Family Serrivomeridae. In: Böhlke EB (ed) Fishes of the western North Atlantic. Sears Foundation for Marine Research, New Haven, pp 613–627

Turingan RG, Wainwright PC, Hensley DA (1995) Interpopulation variation in prey use and feeding biomechanics in Caribean triggerfishes. Oecologia 102:296–304

Van Wassenbergh S, Aerts P, Adriaens D, Herrel A (2005) A dynamical model of mouth closing movements in clariid catfishes: the role of enlarged jaw adductors. J Theor Biol 234:49–65. https://doi.org/10.1016/j.jtbi.2004.11.007

Van Wassenbergh S, Herrel A, Adriaens D, Aerts P (2004) Effects of jaw adductor hypertrophy on buccal expansions during feeding of air breathing catfishes (Teleostei, Clariidae). Zoomorphology 123:81–93. https://doi.org/10.1007/s00435-003-0090-3

Wang CH, Kuo CH, Mok HK, Lee SC (2003) Molecular phylogeny of elopomorph fishes inferred from mitochondrial 12S ribosomal RNA sequences. Zool Scr 32:231–241. https://doi.org/10.1046/j.1463-6409.2003.00114.x

Westneat MW (1994) Transmission of force and velocity in the feeding mechanisms of labrid fishes (Teleostei, Perciformes). Zoomorphology 114:103–118

Westneat MW (2004) Evolution of levers and linkages in the feeding mechanisms of fishes. Integr Comp Biol 44(5):378–389. https://doi.org/10.1093/icb/44.5.378

Westneat MW (2007) Twice bitten. Nature 449:33–34. https://doi.org/10.1038/449033b

Winterbottom R (1974) A descriptive synonymy of the striated muscles of the Teleostei. Proc Acad Natl Sci Phila 125:225–317

Young RF, Winn HE (2003) Activity patterns, diet, and shelter site use for two species of moray eels, *Gymnothorax moringa* and *Gymnothorax vicinus*, in Belize. Copeia 2003(1):44–55

Yukihira H, Shibuno T, Hashimoto H, Gushima K (1994) Feeding habits of moray eels (Pisces: Muraenidae) at Kuchierabujima. Journal of the Faculty of Applied Biological Science - Hiroshima University (Japan) 33:159–166